

# Event-plane flow analysis without non-flow effects

Ante Bilandzic,<sup>1</sup> Naomi van der Kolk,<sup>1</sup> Jean-Yves Ollitrault,<sup>2</sup> and Raimond Snellings<sup>1</sup>

<sup>1</sup>*NIKHEF, Kruislaan 409, 1098 SJ Amsterdam, The Netherlands*

<sup>2</sup>*Institut de Physique Théorique, CEA-Saclay, F-91191 Gif-sur-Yvette cedex*

(Dated: August 31, 2009)

The event-plane method, which is widely used to analyze anisotropic flow in nucleus-nucleus collisions, is known to be biased by nonflow effects, especially at high  $p_t$ . Various methods (cumulants, Lee-Yang zeroes) have been proposed to eliminate nonflow effects, but their implementation is tedious, which has limited their application so far. In this paper, we show that the Lee-Yang-zeroes method can be recast in a form similar to the standard event-plane analysis. Nonflow correlations are eliminated by using the information from the length of the flow vector, in addition to the event-plane angle. This opens the way to improved analyses of elliptic flow and azimuthally-sensitive observables at RHIC and LHC.

PACS numbers: 25.75.Ld, 25.75.Gz, 05.70.Fh

## I. INTRODUCTION

Since elliptic flow has been seen at RHIC [1–3], it has become a crucial observable for our understanding of the system created in heavy-ion collisions. Anisotropic flow is most often analyzed using the event-plane method [4]. These analyses are plagued by systematic errors due to nonflow effects [5]. Nonflow effects are particularly large at high  $p_t$  [6], where they are likely to originate from jet-like (hard) correlations; they are expected to be even larger at the LHC. The purpose of this paper is to show that nonflow effects can be avoided at the expense of a slight modification of the event-plane method.

Anisotropic flow of an outgoing particle of a given type, in a given phase-space window, is defined as its azimuthal correlation with the reaction plane [7]

$$v_n \equiv \langle \cos(n(\phi - \Phi_R)) \rangle \quad (1)$$

where  $n$  is an integer ( $v_1$  is *directed* flow,  $v_2$  is *elliptic* flow),  $\phi$  denotes the azimuth of the particle under study,  $\Phi_R$  the azimuth of the reaction plane, and angular brackets denote an average over particles and events. Since  $\Phi_R$  is not known experimentally,  $v_n$  cannot be measured directly.

The most commonly used method to estimate  $v_n$  is the event-plane method [4]. In each event, one constructs an estimate of the reaction plane  $\Phi_R$ , the “event plane”  $\Psi_R$  [8]. The anisotropic flow coefficients are then estimated as

$$v_n\{\text{EP}\} \equiv \frac{1}{R} \langle \cos(n(\phi - \Psi_R)) \rangle, \quad (2)$$

where  $R = \langle \cos(n(\Psi_R - \Phi_R)) \rangle$  is the event-plane resolution, which corrects for the difference between  $\Psi_R$  and  $\Phi_R$ . This resolution is determined in each centrality class through a standard procedure [9].

The analogy between Eq. (2) with Eq. (1) makes the method rather intuitive, but its practical implementation has a few subtleties:

- One must remove autocorrelations: the particle under study should not be used in defining the event

plane, otherwise there is a trivial correlation between  $\phi$  and  $\Psi_R$  [8]. This means in practice that one must keep track of which particles have been used in defining the event plane, so as to remove them if necessary.

- Nonflow correlations between the particle under study and the event plane must be avoided. This cannot be done in a systematic way, but rapidity gaps are believed to largely suppress nonflow effects [3, 10].
- Event-plane flattening procedures must be implemented to correct for azimuthal asymmetries of the detector acceptance [4].

A systematic way of eliminating nonflow effects is to use improved methods such as cumulants [11] or Lee-Yang zeroes [12]. Cumulants have been used at SPS [13] and RHIC [6, 14] but their implementation is tedious. In this paper, we show that the method of flow analysis based on Lee-Yang zeroes can be recast in a form similar to the event-plane method. Specifically, Eq. (2) is replaced with

$$v_n\{\text{LYZ}\} \equiv \langle W_R \cos(n(\phi - \Psi_R)) \rangle, \quad (3)$$

where  $\Psi_R$  is the same as in Eq. (2), and  $W_R$  is a new quantity, the *event weight*, which depends on the length of the flow vector. The advantage of this improved event-plane method over the standard event-plane method is that *both autocorrelations and nonflow effects* are automatically removed.

The paper is organized as follows. In Sec. II, we describe the method for a detector with perfect azimuthal symmetry, and we explain why it automatically gets rid of autocorrelations and nonflow correlations, in contrast to the standard event-plane method. Readers interested in applying the method should jump to Appendix A, which describes the recommended practical implementation, taking into account anisotropies in the detector acceptance. In Sec. III, we present results of Monte-Carlo

simulations. Lee-Yang zeroes are compared to 2- and 4-particle cumulants. Sec. IV concludes with a discussion of where the method should be applicable, and of its limitations.

## II. DESCRIPTION OF THE METHOD

### A. The flow vector

The first step of the flow analysis is to evaluate, for each event, the flow vector of the event. It is a two-dimensional vector  $\mathbf{Q} = (Q_x, Q_y)$  defined as

$$\begin{aligned} Q_x &= Q \cos(n\Psi_R) \equiv \sum_{j=1}^M w_j \cos(n\phi_j) \\ Q_y &= Q \sin(n\Psi_R) \equiv \sum_{j=1}^M w_j \sin(n\phi_j), \end{aligned} \quad (4)$$

where the sum runs over all detected particles,  $M$  is the observed multiplicity of the event,  $\phi_j$  are the azimuthal angles of the particles measured with respect to a fixed direction in the laboratory. The coefficients  $w_j$  in Eq. (4) are weights depending on transverse momentum, particle mass and rapidity. The best weight, which minimizes the statistical error (or, equivalently, maximizes the resolution) is  $v_n$  itself,  $w_j(p_T, y) \propto v_n(p_T, y)$  [15]. A reasonable choice for elliptic flow at RHIC (and probably LHC) is  $w = p_T$ .

Lee-Yang zeroes use the projection of the flow vector onto a fixed, arbitrary direction making an angle  $n\theta$  with respect to the  $x$ -axis. We denote this projection by  $Q^\theta$ :

$$Q^\theta \equiv Q_x \cos n\theta + Q_y \sin n\theta = Q \cos(n(\Psi_R - \theta)). \quad (5)$$

### B. Integrated flow

The first step of the analysis is to measure the integrated flow  $V_n$ , defined as the average value of the projection of  $\mathbf{Q}$  onto the true reaction plane:

$$V_n \equiv \langle Q \cos(n(\Psi_R - \Phi_R)) \rangle \quad (6)$$

where angular brackets denote an average over events.

We define the complex-valued function:

$$G^\theta(r) \equiv \frac{1}{N_{\text{evts}}} \sum_{\text{events}} e^{irQ^\theta} \quad (7)$$

The modulus  $|G^\theta(r)|$  can be plotted as a function of  $r$  for positive  $r$ . In the case where collective flow is present, this modulus has a sharp minimum, compatible with 0 within statistical errors [16]. This is the Lee-Yang zero, which is determined by finding the first minimum numerically. We denote its value by  $r^\theta$ . The estimate of the integrated flow is then defined by

$$V_n = \frac{j_{01}}{r^\theta}, \quad (8)$$

where  $j_{01} \simeq 2.40483$  is the first zero of the spherical Bessel function  $J_0(x)$ .

Please note that the above procedure only makes use of the projection of the flow vector onto an arbitrary direction  $\theta$ . For a perfect detector, azimuthal symmetry ensures that  $r^\theta$  is independent of  $\theta$ , up to statistical errors. In practice, however, it is recommended to repeat the analysis for several values of  $\theta$  (see Appendix A).

### C. Event weight

Once  $r^\theta$  is determined, the event weight is defined by

$$W_R \equiv \frac{1}{C} J_1(r^\theta Q), \quad (9)$$

where  $J_1(x)$  is the spherical Bessel function of first order,  $Q$  is the length of the flow vector, and  $C$  is a normalization constant which is the same for all events in the centrality class. This constant is determined by requiring that the projection of the flow vector  $\mathbf{Q}$  onto the reaction plane corresponds to the integrated flow  $V_n$ , defined by Eq. (6). This gives the condition

$$(W_R Q) = V_n. \quad (10)$$

Inserting Eqs. (8) and (9), we obtain

$$C = \frac{1}{j_{01}} \langle r^\theta Q J_1(r^\theta Q) \rangle \quad (11)$$

where angular brackets denote an average over events.

This normalization constant can be shown to be related to the resolution parameter  $\chi$  used in the standard event-plane analysis (see Appendix A 3 for a precise definition):

$$C = \exp\left(-\frac{j_{01}^2}{4\chi^2}\right) J_1(j_{01}). \quad (12)$$

Fig. 1 displays the weight  $W_R$  as a function of the length of the flow vector  $Q$ , together with the probability distribution of  $Q$ , for two values of the resolution parameter. The normalized distribution of  $Q$  is [5]

$$\frac{dN}{dQ} = \frac{2\chi^2 Q}{V_n^2} \exp\left(-\chi^2 \left(\frac{Q^2}{V_n^2} + 1\right)\right) I_0\left(\frac{2\chi^2 Q}{V_n}\right). \quad (13)$$

For  $\chi \gg 1$ , this distribution is a narrow peak centered at  $Q = V_n$ . The weight defined by Eqs. (9) and (12) is then close to 1 for all events. If  $\chi$  is smaller, the distribution of  $Q$  is correspondingly wider, and  $W_R$  is negative for some events. These negative weights are required in order to subtract nonflow effects, as will be explained in Sec. II D. On the other hand, they also subtract part of the flow. In order to compensate for this effect, the global normalization of the weight increases when  $\chi$  decreases (compare the curves in the top and bottom panels in Fig. 1). This qualitatively explains the  $\chi$  dependence in Eq. (12).

The weight (9) vanishes linearly at  $Q = 0$ . This is physically intuitive. The idea of the flow vector is that

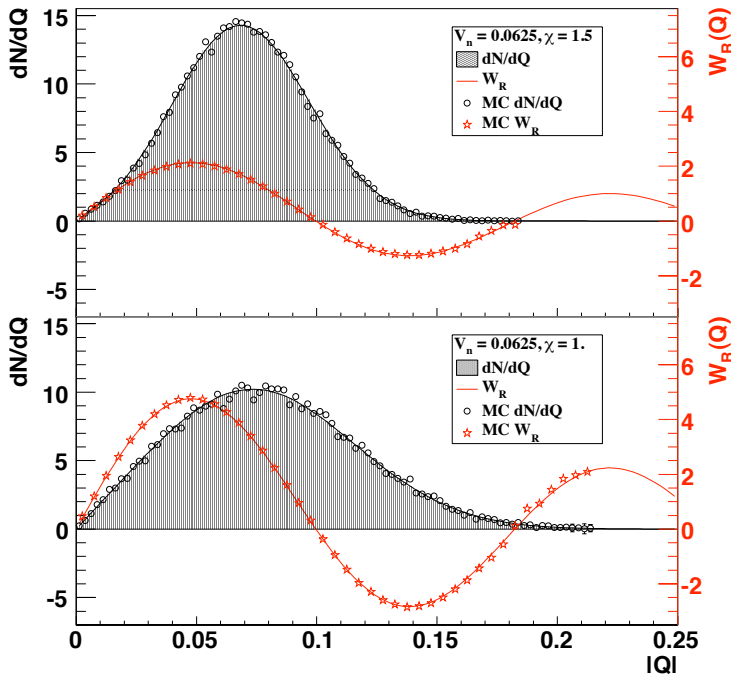


FIG. 1: (color online) Shaded area: probability distribution of  $Q$ , Eq. (13), with  $V_n = 0.0625$  (see Sec. III). Open circles: histograms of the distribution of  $Q$  obtained in the Monte-Carlo simulation of Sec. III, following the procedure detailed in Appendix A. Solid curve: weight  $W_R$  defined by Eqs. (9) and (12). Stars: weights obtained in Sec. III. Top:  $\chi = 1.5$ , corresponding to a resolution  $R = 0.86$  in the standard analysis (see Eq. (2)). Bottom:  $\chi = 1$ , corresponding to a resolution  $R = 0.71$ . This is the typical value for a semi-central Au-Au collision at RHIC analyzed by the STAR TPC [6].

by summing over all particles, one increases the relative weight of collective flow over individual, random motion of the particles. If the flow vector is small in an event, it means that the random motion hides the collective motion in this particular event, which is therefore of little use for the flow analysis.

#### D. Autocorrelations and nonflow effects

We now explain why the method is insensitive to autocorrelations and nonflow effects. We consider the situation where there is collective flow in the system, so that  $v_n$  is non-zero for most of the particles. Next, we assume that the particle under study does not take part in collective flow, i.e., it has  $v_n = 0$ ; on the other hand, it may be correlated with a few other particles (for instance if they belong to the same jet). Such nonflow correlations usually result in  $v_n\{\text{EP}\} \neq 0$  (generally  $> 0$  for intra-jet correlations). By contrast, our improved estimate  $v_n\{\text{LYZ}\}$  vanishes, as we now show.

We separate the flow vector, Eq. (4), into a flow part

$\mathbf{Q}_f$ , involving particles which contribute to collective flow, and a non-flow part  $\mathbf{Q}_{\text{nf}}$ , involving the particle under interest (autocorrelations) and the few particles which are correlated to it, but do not contribute to collective flow:

$$\mathbf{Q} = \mathbf{Q}_f + \mathbf{Q}_{\text{nf}}. \quad (14)$$

We further assume that the flow and the nonflow part are uncorrelated.

Eqs. (3) and (9) define our estimate of  $v_n$  as

$$v_n\{\text{LYZ}\} \equiv \frac{1}{C} \langle J_1(r^\theta Q) \cos(n(\phi - \Psi_R)) \rangle. \quad (15)$$

We rewrite the Bessel function as an integral over angles [17]

$$J_1(r^\theta Q) \cos(n(\phi - \Psi_R)) = -i \int_0^{2\pi} \frac{d\theta}{2\pi} e^{ir^\theta Q^\theta} \cos(n(\phi - \theta)), \quad (16)$$

with  $Q^\theta$  defined by Eq. (5). Since the flow vector appears in an exponential, the flow and nonflow contributions to Eq. (15) can be written as a product of two independent factors:

$$v_n\{\text{LYZ}\} = -\frac{i}{C} \int_0^{2\pi} \frac{d\theta}{2\pi} \langle e^{ir^\theta Q_f^\theta} \rangle \langle e^{ir^\theta Q_{\text{nf}}^\theta} \cos(n(\phi - \theta)) \rangle. \quad (17)$$

We then use again the assumption that the flow and nonflow part are uncorrelated to write

$$\langle e^{ir^\theta Q^\theta} \rangle = \langle e^{ir^\theta Q_f^\theta} \rangle \langle e^{ir^\theta Q_{\text{nf}}^\theta} \rangle. \quad (18)$$

Now,  $\langle e^{ir^\theta Q^\theta} \rangle = 0$  by definition of the Lee-Yang zero  $r^\theta$ , up to statistical fluctuations. This means that one of the two factors in the right-hand side of Eq. (18) vanishes. Since it is the flow which produces the zero, it means that  $\langle e^{ir^\theta Q_f^\theta} \rangle = 0$ . Inserting into Eq. (17), we find

$$v_n\{\text{LYZ}\} = 0, \quad (19)$$

up to statistical fluctuations. This completes our proof that the method is not biased by autocorrelations and nonflow effects.

### III. SIMULATIONS

$N = 28\,000$  events were simulated with a Monte-Carlo program dubbed GeVSim[18]. In GeVSim the  $v_2$  and the particle yield as function of transverse momentum and pseudorapidity can be set with a user-defined parameterization. For these simulations events were generated using a linear dependence of  $v_2(p_t)$  in the range 0–2 GeV/c, above 2 GeV/c the  $v_2(p_t)$  was set constant. The average elliptic flow is  $\langle v_2 \rangle = 0.0625$ . We then reconstructed  $v_2(p_t)$  from the simulated events using several methods: the Lee-Yang-zeros method described in

Appendix A, 2- and 4-particle cumulants [11]. The corresponding estimates of  $v_2$  are denoted by  $v_2\{\text{LYZ}\}$ ,  $v_2\{2\}$  and  $v_2\{4\}$ , respectively.  $v_2\{2\}$  is generally close to  $v_2$  from the traditional event-plane method; both are biased by nonflow effects. On the other hand,  $v_2\{4\}$  is expected to be close to  $v_2\{\text{LYZ}\}$ , with the bias from nonflow effects subtracted. The weight  $w_j$  in Eq. (4) was chosen identically  $1/M$  for all particles, with  $M$  the event multiplicity, so that the integrated flow  $V_n$  defined by Eq. (1) coincides with the average elliptic flow, i.e.,  $V_n = 0.0625$ . The analysis was repeated twice by varying the multiplicity  $M$  used in the flow analysis: the values 256 and 576 were used, so as to achieve a resolution of  $\chi = 1$  and 1.5. [31]

Fig. 2 shows the generated (input)  $v_2(p_t)$  together with the reconstructed  $v_2(p_t)$  using cumulants and Lee-Yang zeroes for  $\chi = 1$ . The upper panel shows the results in the case where all correlations are due to flow. In this case, all three methods yield the correct  $v_2(p_t)$  and  $\langle v_2 \rangle$  within statistical uncertainties (see Table I), which are twice larger for  $v_2\{4\}$  and  $v_2\{\text{LYZ}\}$  than for  $v_2\{2\}$  (see Sec. A 3).

In the lower panel, simulations are shown which include nonflow effects. Nonflow correlations are introduced by using each input track twice, roughly imitating the effect of resonance decays or track splitting in a detector. Experiments at RHIC have shown [6] that nonflow effects are larger at high- $p_t$  (probably due to jet-like correlations), and a realistic simulation of nonflow effects should take into account this  $p_t$  dependence. Our simplified implementation, which does not, is not realistic. It is merely an illustration of the impact of nonflow effects on the flow analysis. Fig. 2 shows that due to nonflow effects, the method based on two-particle cumulants ( $v_2\{2\}$ ) overestimates the average elliptic flow  $\langle v_2 \rangle$ . The error on the average elliptic flow is larger than 20% (see Table I, right column). The transverse-momentum dependence of  $v_2(p_t)$  is also not correct, with an excess at low  $p_t$  by 0.03. By contrast, the results from 4-particle cumulants ( $v_2\{4\}$ ) and Lee-Yang zeroes ( $v_2\{\text{LYZ}\}$ ) are, within statistical uncertainties, in agreement with the true generated flow distribution. This shows that the method presented in this paper is able to get rid of nonflow effects.

TABLE I: Value of the average elliptic flow  $\langle v_2 \rangle$  reconstructed using different methods with and without nonflow effects in the simulated data. The input value is  $\langle v_2 \rangle = 0.0625$ .

Method	Flow only	Flow+nonflow
$v_2\{2\}$	$0.0626 \pm 0.0003$	$0.0764 \pm 0.0004$
$v_2\{4\}$	$0.0624 \pm 0.0005$	$0.0627 \pm 0.0007$
$v_2\{\text{LYZ}\}$	$0.0626 \pm 0.0005$	$0.0629 \pm 0.0007$

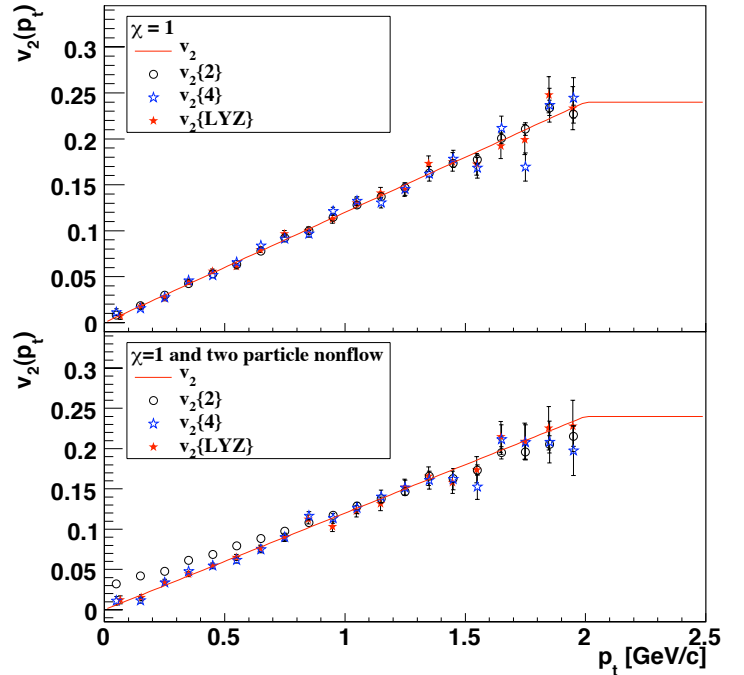


FIG. 2: Differential elliptic flow  $v_2(p_t)$  reconstructed using different methods: the line is the input  $v_2$ . The upper, lower panel shows the obtained  $v_2(p_t)$  for the different methods without and with nonflow present, respectively.

#### IV. DISCUSSION

Two effects limit the accuracy of flow analyses at high energy: nonflow effects and eccentricity fluctuations [19, 20]. The method presented in this paper is an improved event-plane method, which eliminates the first source of uncertainty, nonflow effects. It has been recently argued [21] that cumulants (and therefore Lee-Yang zeroes, which corresponds to the limit of large-order cumulants) also eliminate eccentricity fluctuations [19, 20]. However, a recent detailed study [22] shows that even with cumulants, there may remain large effects of fluctuations in central collisions and/or small systems. This issue deserves more detailed investigations.

Letting aside the question of fluctuations, we now discuss which method of flow analysis should be used, depending on the situation. There are three main classes of methods: the standard event-plane method [4], four-particle cumulants [11], and the Lee-Yang-zeroes method presented in this paper. When the standard event-plane method is used, nonflow effects and eccentricity fluctuations are generally the main sources of uncertainty on  $v_n$ , and they dominate over statistical errors. The magnitude of this uncertainty is at least 10% at RHIC in semi-central collisions; it is larger for more central or more peripheral collisions, and also larger at high  $p_t$ . Unless statistical errors are of comparable magnitude as errors from nonflow effects, cumulants or Lee-Yang zeroes should be preferred

over the standard method.

The advantages of Lee-Yang zeroes over 4-particle cumulants are: 1) They are easier to implement. 2) They further reduce the error from nonflow effects. 3) Effects of azimuthal asymmetries in the detector acceptance are much smaller. 4) The statistical error is slightly smaller if the resolution parameter  $\chi > 1$ . For  $\chi = 0.8$ , the error is only 35% larger with Lee-Yang zeroes than with 4-particle cumulants (and 4 times larger than with the event-plane method).

Our recommendation is that Lee-Yang zeroes should be used as soon as  $\chi > 0.8$ . For small values of  $\chi$ , typically  $\chi < 0.6$ , statistical errors on Lee-Yang zeroes blow up exponentially, which rules out the method; the statistical error on 4-particle cumulants also increases but more mildly, and their validity extends down to lower values of the resolution if very large event statistics is available.

A limitation of the present method is that it does not apply to mixed harmonics: this means that it cannot be used to measure  $v_1$  and  $v_4$  at RHIC and LHC using the event plane from elliptic flow [23]. Note that  $v_1$  can in principle be measured using Lee-Yang zeroes [24] using the “product” generating function, but this method cannot be recast in the form of an improved event-plane method. Higher harmonics such as  $v_4$  also have a sensitivity to autocorrelations and nonflow effects, which is significantly reduced by using the product generating function [11].

Although we have only explained how to analyze the anisotropic flow of individual particles, it is straightforward to extend the method to azimuthally dependent correlations [25, 26]. The only complication is that the azimuthal distribution of particle pairs generally involves *sine* terms [27], in addition to the *cosine* terms of Eq. (1). These terms are simply obtained by replacing  $\cos$  with  $\sin$  in Eq. (3).

In conclusion, we have presented an improved event-plane method for the flow analysis, which automatically corrects for autocorrelations and nonflow effects. As in the standard method, each event has its *event plane*  $\Psi_R$ , an estimate of the reaction plane, which is the same as for the standard method, except for technical details in the practical implementation. The trick which removes autocorrelations and nonflow effects is that there is in addition an *event weight*. Anisotropic flow  $v_n$  is then estimated as a *weighted* average of  $\cos(n(\phi - \Psi_R))$ . A straightforward application of this method would be to measure jet production with respect to the reaction plane at LHC. With the traditional event-plane method, such a measurement would require to subtract particles belonging to the jet from the event plane; in addition, strong nonflow correlations are expected within a jet, which would bias the analysis.

## Acknowledgments

JYO thanks Yiota Foka for a discussion which motivated this work.

## APPENDIX A: PRACTICAL IMPLEMENTATION

Before we describe the implementation of the method, let us mention that there are in fact two Lee-Yang-zeroes methods, depending on how the generating function is defined: the “sum generating function” makes explicit use of the flow vector [16], while the “product generating function” [28] is constructed using the azimuthal angles of individual particles, and cannot be expressed simply in terms of the flow vector. Cumulants also exist in both versions, the “sum” [15] and the “product” [11]. For Lee-Yang zeroes, both the sum and the product give essentially the same result for the lowest harmonic [29]: the difference between results from the two methods is significantly less than the statistical error. On the other hand, the product generating function is significantly better than the sum generating function if one analyzes  $v_4$  or  $v_1$  [24] using mixed harmonics. The method described below is strictly equivalent to the sum generating function, although expressed in different terms. On the other hand, the product generating function cannot be recast in a form similar to the event-plane method, and will not be used here.

The method a priori requires two passes through the data, which are described in Sec. A 1 and Sec. A 2.

### 1. First pass: locating the zeroes

As with other flow analyses, one must first select events in some centrality class. The whole procedure described below must be carried out independently for each centrality class.

The flow vector  $(Q_x, Q_y)$  is defined by Eq. (4). In contrast to the standard event-plane method, no flattening procedure is required to make the distribution of  $\mathbf{Q}$  isotropic. Corrections for azimuthal anisotropies in the acceptance, which do not vary significantly in the event sample used, are handled using the procedure described below. We do not define the event plane  $\Psi_R$  as the azimuthal angle of the flow vector, as in Eq. (4). The procedure below defines both the event weight and the event plane.

The analysis uses the projection of the flow vector onto an arbitrary direction, see Eq. (5). In practice, the first pass should be repeated for several equally-spaced values of  $n\theta$  between 0 and  $\pi$ . This reduces the statistical error, 5 values of  $\theta$  suffice, see Eq. A5. For elliptic flow, for instance,  $\theta$  takes the values  $\theta = 0, \pi/10, 2\pi/10, 3\pi/10, 4\pi/10$ .

One first computes the modulus  $|G^\theta(r)|$ , with  $G^\theta$  defined by Eq. (7), as a function of  $r$  for positive  $r$ . One

determines numerically the first minimum of this function. This is the Lee-Yang zero. We denote its value by  $r^\theta$ . It must be stored for each  $\theta$ .

## 2. Second pass: determining the event weight, $w_R$ , and the event plane, $\Psi_R$ .

In the second pass, one computes and stores, for each  $\theta$ , the following complex number:

$$D^\theta \equiv \frac{1}{j_{01} N_{\text{evts}}} \sum_{\text{events}} r^\theta Q^\theta e^{ir^\theta Q^\theta}, \quad (\text{A1})$$

where  $j_{01} \simeq 2.40483$ . Except for statistical fluctuations and asymmetries in the detector acceptance,  $D^\theta$  should be purely imaginary.

For each event, the event weight and the event plane are defined by

$$\begin{aligned} W_R \cos n\Psi_R &\equiv \left\langle \text{Re} \left( \frac{e^{ir^\theta Q^\theta}}{D^\theta} \right) \cos n\theta \right\rangle_\theta \\ W_R \sin n\Psi_R &\equiv \left\langle \text{Re} \left( \frac{e^{ir^\theta Q^\theta}}{D^\theta} \right) \sin n\theta \right\rangle_\theta, \end{aligned} \quad (\text{A2})$$

where  $\text{Re}$  denotes the real part, and angular brackets denote averages over the values of  $\theta$  defined in subsection A1. Our estimate of  $v_n$ , denoted by  $v_n\{\text{LYZ}\}$ , is then defined by Eq. (3).

We now discuss how the angle  $\Psi_R$  defined by Eq. (A2) compares with the event-plane from the standard analysis. First, we note that Eqs. (A2) uniquely determine the angle  $n\Psi_R$  (modulo  $2\pi$ ) only if the sign of  $W_R$  is known. The simplest convention is  $W_R > 0$ . In the simplified implementation described in Sec. II, however, where  $\Psi_R$  coincides with the standard event plane,  $W_R$  defined by Eq. (9) can be negative, because the Bessel function changes sign (see Fig. 1). The convention  $W_R > 0$  then leads to a value of  $n\Psi_R$  which differs from the standard event plane by  $\pi$ , since changing the sign of  $W_R$  amounts to shifting  $n\Psi_R$  by  $\pi$  in Eqs. (A2). This is illustrated in Fig. 3, which shows the distribution of the relative angle between  $\Psi_R$  and the standard event plane in the simulation of  $v_2$  at LHC described in Sec. III. The distribution has two sharp peaks at 0 and  $\pi/2$ . The sign ambiguity produces the peak at  $\pi/2$ . The width of the peaks results from statistical fluctuations. The final result  $v_n\{\text{LYZ}\}$ , given by Eq. (3), does not depend on the sign chosen for  $W_R$ .

If one wishes to have an event-plane as close as possible to the standard event plane, one may choose the following convention. Denoting by  $\Psi_R^{\text{std}}$  the standard event plane, one computes the following quantity:

$$S \equiv W_R \cos n\Psi_R \cos n\Psi_R^{\text{std}} + W_R \sin n\Psi_R \sin n\Psi_R^{\text{std}}, \quad (\text{A3})$$

where  $W_R \cos n\Psi_R$  and  $W_R \sin n\Psi_R$  are defined by Eq. (A2). The sign of  $W_R$  is then chosen as the sign

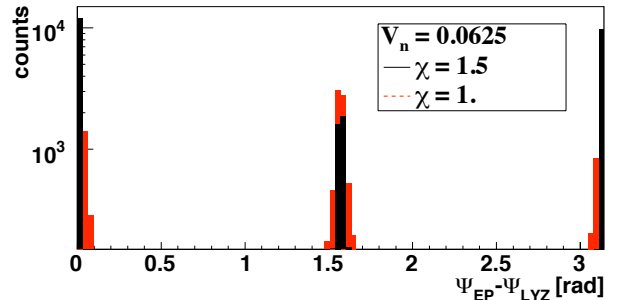


FIG. 3: Distribution of the relative angle between the event plane  $\Psi_R$  defined by Eq. (A2), with  $W_R > 0$ , and the standard event plane, for the reconstruction shown in Fig. 2.

of  $S$ , which ensures that  $n\Psi_R - n\Psi_R^{\text{std}}$  lies between  $-\pi/2$  and  $\pi/2$ .

The procedure described in this Appendix differs from the procedure described in Sec. II only in the case of non-uniform acceptance. This agreement can be seen in Fig. 1, which displays a comparison between the two. The solid line corresponds to the weight defined in Sec. II (Eqs. (9) and (12)), while the stars corresponds to the weight defined by Eq. (A2), as implemented in the Monte-Carlo simulation presented in Sec. III. The agreement is very good. This agreement can also be seen directly on the equations. If the detector has perfect azimuthal symmetry,  $r^\theta$  and  $D^\theta$  in Eq. (A2) are independent of  $\theta$ , up to statistical fluctuations. Neglecting these fluctuations, replacing  $Q^\theta$  with Eq. (5) and integrating over  $\theta$ , one easily recovers Eq. (9). If there are azimuthal asymmetries in the detector acceptance, on the other hand, they are automatically taken care of by Eq. (A2). The fact that one first projects the flow vector onto a fixed direction  $\theta$  is essential (for a related discussion, see [30]).

## 3. Statistical errors

The statistical error strongly depends on the resolution parameter [9]  $\chi$ , which is closely related to the reaction plane resolution in the event-plane analysis. It is given by

$$\chi = \frac{V_n}{\sqrt{\langle Q_x^2 + Q_y^2 \rangle - \langle Q_x \rangle^2 - \langle Q_y \rangle^2 - V_n^2}}. \quad (\text{A4})$$

In this equation,  $V_n$  is given by Eq. (8), averaged over  $\theta$  to minimize the statistical dispersion. The average values  $\langle Q_x \rangle$ ,  $\langle Q_y \rangle$ ,  $\langle Q_x^2 \rangle$  and  $\langle Q_y^2 \rangle$  must be computed in the first pass through the data. Please note that  $\langle Q_x \rangle$  and  $\langle Q_y \rangle$  vanish for a symmetric detector: they are acceptance corrections.

The price to pay for the elimination of nonflow effects is an increased statistical error. This increase is very

modest if  $\chi$  is larger than 1: If  $\chi = 1.5$ , the error is only 25% larger than with the standard event-plane method. If  $\chi = 1$ , it is larger by a factor 2. If  $\chi = 0.6$ , it is 20 times larger. This prevents the application of Lee-Yang zeroes in practice for  $\chi$  smaller than 0.6.

We now recall the formulas [12] which determine the statistical error  $\delta v_n^{\text{stat}}$  on  $v_n\{\text{LYZ}\}$ :

$$(\delta v_n^{\text{stat}})^2 = \frac{1}{4N'J_1(j_{01})^2p} \sum_{k=0}^{p-1} \cos\left(\frac{k\pi}{p}\right) \times \left[ \exp\left(\frac{j_{01}^2}{2\chi^2} \cos\left(\frac{k\pi}{p}\right)\right) J_0\left(2j_{01} \sin\left(\frac{k\pi}{2p}\right)\right) \right]$$

$$- \exp\left(-\frac{j_{01}^2}{2\chi^2} \cos\left(\frac{k\pi}{p}\right)\right) J_0\left(2j_{01} \cos\left(\frac{k\pi}{2p}\right)\right) \right] \quad (\text{A5})$$

where  $N'$  denotes the number of objects one correlates to the event plane, whatever they are (jets, individual particles), and  $p$  is the number of equally-spaced values of  $\theta$  used in the analysis (see above). The larger  $p$ , the smaller the error. The recommended value is  $p = 5$ , because larger values do not significantly reduce the error. This equation shows that the statistical error diverges exponentially when  $\chi$  is small.

- 
- [1] K. H. Ackermann *et al.* [STAR Collaboration], Phys. Rev. Lett. **86**, 402 (2001) [arXiv:nucl-ex/0009011].
- [2] B. B. Back *et al.* [PHOBOS Collaboration], Phys. Rev. Lett. **89**, 222301 (2002) [arXiv:nucl-ex/0205021].
- [3] S. S. Adler *et al.* [PHENIX Collaboration], Phys. Rev. Lett. **91**, 182301 (2003) [arXiv:nucl-ex/0305013].
- [4] A. M. Poskanzer and S. A. Voloshin, Phys. Rev. C **58**, 1671 (1998) [arXiv:nucl-ex/9805001].
- [5] J. Y. Ollitrault, Nucl. Phys. A **590**, 561C (1995).
- [6] J. Adams *et al.* [STAR Collaboration], Phys. Rev. C **72**, 014904 (2005) [arXiv:nucl-ex/0409033].
- [7] S. Voloshin and Y. Zhang, Z. Phys. C **70**, 665 (1996) [arXiv:hep-ph/9407282].
- [8] P. Danielewicz and G. Odyniec, Phys. Lett. B **157**, 146 (1985).
- [9] J. Y. Ollitrault, arXiv:nucl-ex/9711003.
- [10] S. A. Voloshin [STAR Collaboration], AIP Conf. Proc. **870**, 691 (2006) [arXiv:nucl-ex/0610038].
- [11] N. Borghini, P. M. Dinh and J. Y. Ollitrault, Phys. Rev. C **64**, 054901 (2001) [arXiv:nucl-th/0105040]; arXiv:nucl-ex/0110016.
- [12] R. S. Bhalerao, N. Borghini and J. Y. Ollitrault, Nucl. Phys. A **727**, 373 (2003) [arXiv:nucl-th/0310016].
- [13] C. Alt *et al.* [NA49 Collaboration], Phys. Rev. C **68**, 034903 (2003) [arXiv:nucl-ex/0303001].
- [14] C. Adler *et al.* [STAR Collaboration], Phys. Rev. C **66**, 034904 (2002) [arXiv:nucl-ex/0206001].
- [15] N. Borghini, P. M. Dinh and J. Y. Ollitrault, Phys. Rev. C **63**, 054906 (2001) [arXiv:nucl-th/0007063].
- [16] R. S. Bhalerao, N. Borghini and J. Y. Ollitrault, Phys. Lett. B **580**, 157 (2004) [arXiv:nucl-th/0307018].
- [17] S. A. Voloshin, arXiv:nucl-th/0606022.
- [18] S. Radomski and Y. Foka, ALICE NOTE 2002-31; <http://www.gsi.de/forschung/kp/kp1/gevsim.html>
- [19] M. Miller and R. Snellings, arXiv:nucl-ex/0312008.
- [20] B. Alver *et al.* [PHOBOS Collaboration], Phys. Rev. Lett. **98**, 242302 (2007) [arXiv:nucl-ex/0610037].
- [21] S. A. Voloshin, A. M. Poskanzer, A. Tang and G. Wang, arXiv:0708.0800 [nucl-th].
- [22] B. Alver *et al.*, arXiv:0711.3724 [nucl-ex].
- [23] J. Adams *et al.* [STAR Collaboration], Phys. Rev. Lett. **92**, 062301 (2004) [arXiv:nucl-ex/0310029].
- [24] N. Borghini and J. Y. Ollitrault, Nucl. Phys. A **742**, 130 (2004) [arXiv:nucl-th/0404087].
- [25] J. Adams *et al.* [STAR Collaboration], Phys. Rev. Lett. **93**, 252301 (2004) [arXiv:nucl-ex/0407007].
- [26] J. Bielcikova, S. Esumi, K. Filimonov, S. Voloshin and J. P. Wurm, Phys. Rev. C **69**, 021901 (2004) [arXiv:nucl-ex/0311007].
- [27] N. Borghini and J. Y. Ollitrault, Phys. Rev. C **70**, 064905 (2004) [arXiv:nucl-th/0407041].
- [28] N. Borghini, R. S. Bhalerao and J. Y. Ollitrault, J. Phys. G **30**, S1213 (2004) [arXiv:nucl-th/0402053].
- [29] N. Bastid *et al.* [FOPI Collaboration], Phys. Rev. C **72**, 011901 (2005) [arXiv:nucl-ex/0504002].
- [30] I. Selyuzhenkov and S. Voloshin, arXiv:0707.4672 [nucl-th].
- [31] The resolution parameter depends on the average elliptic flow  $\langle v_2 \rangle$ , and on the event multiplicity  $M$ . It is simply  $\chi = \langle v_2 \rangle \sqrt{M}$  when all particles are given the same weight in Eq. (4).